SURFACE COMPOSITION AND MINERALOGY OF THE APENNINE BENCH FORMATION. S. N. Valencia[1,2], R. N. Watkins[3], D. P. Moriarty III[1,2], B. L. Jolliff[4], and N. E. Petro[2]. [1]University of Maryland, Department of Astronomy, College Park, MD 20742. [2]NASA Goddard Space Flight Center, Planetary Geology, Geophysics, and Geochemistry Laboratory, Greenbelt, MD 20771 (sarah.n.valencia@nasa.gov). [3]Planetary Science Institute, 1700 E Fort Lowell Rd., Tucson, AZ 85719. [4]Washington University, Department of Earth and Planetary Sciences St. Louis, MO 63130.

Introduction: The Apennine Bench Formation (ABF) is a geologic unit in southeast Imbrium basin on the Moon, differentiated from the surrounding units by its distinct chemistry and surface properties [1]. Compared to the surrounding mare, ejecta (primarily from Archimedes crater), and the Apennine Mountains, the ABF is intermediate in topography and surface roughness [2]. Additionally, the ABF has comparatively moderate FeO concentrations (~12.3 wt. % avg.) and elevated Th concentrations (8.7 ppm avg.) [2]. Together, this chemistry suggests that the ABF is composed of KREEP (a chemical component concentrated in the final dregs of the cooling lunar magma ocean) basalt, which would make it the only known large surface expression of KREEP basalt on the Moon [e.g. 3-5].

Here we examine the surface composition of the ABF and surrounding geologic units using data from the Lunar Reconnaissance Orbiter Camera (LROC) and the Moon Mineralogy Mapper (M^3), which flew aboard the Chandrayaan-1 mission, with the aim of improving our understanding of the surface properties and composition of the ABF.

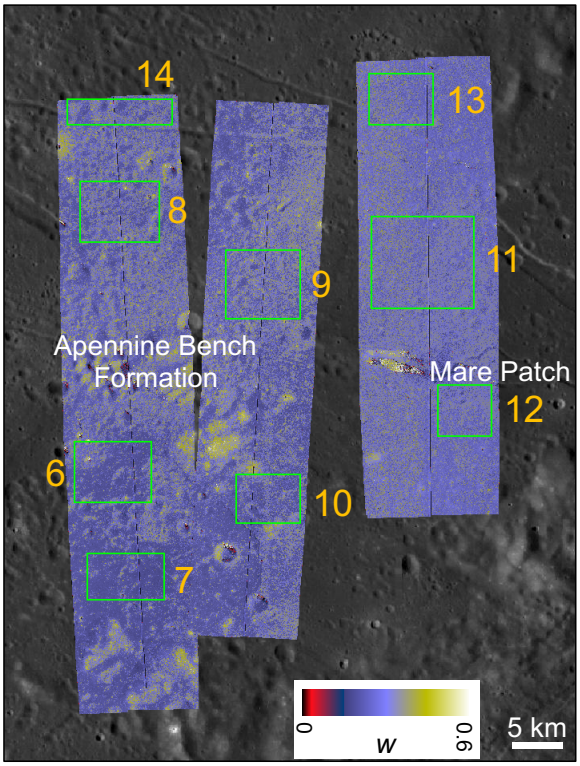

Figure 1. Single scattering albedo (*w*) map of the ABF and nearby mare patch covering a subset of ROIs in the study region. The ABF has lower mafic content, on average, than the mare patch, and higher mafic content than Archimedes ejecta, as reflected by *w* values.

Methods: We use the USGS's Integrated Software for Imagers and Spectrometers to process LROC Narrow Angle Camera (NAC) images, resampled to match the resolution of NAC-derived Digital Terrain Models (DTMs; 5mpp). To assess photometric differences, and therefore mineralogical variations within ABF, we produce Hapke photometric parameter maps following the methods of [7] (Fig. 1). This method allows us to correct for local topography and viewing geometries, thereby reducing the effects of solar illumination and slopes on the derived photometric parameters. The parameter of interest for this work is the single scattering albedo, *w*, which is largely controlled by composition.

We selected M^3 images from the Optical Period 1b (OP1B) and applied photometric and ground truth corrections [8,9]. We processed M^3 images using ENVI (Exelis) to apply a parabolic absorption fit after removing a two-part linear continuum (PLC), following the methods of [10]. We collected spectra (3×3 pixel average) from representative regions of ABF and mare. The output of the PLC method includes estimated absorption band depth (EBD) and estimated band center wavelength position (EBC). The EBD and EBC parameters are used to characterize the 1 μm and 2 μm absorption features. For the lunar surface, the 1 μm and 2 μm absorption features are diagnostic of mafic mineral content and pyroxene composition [e.g., 10-13].

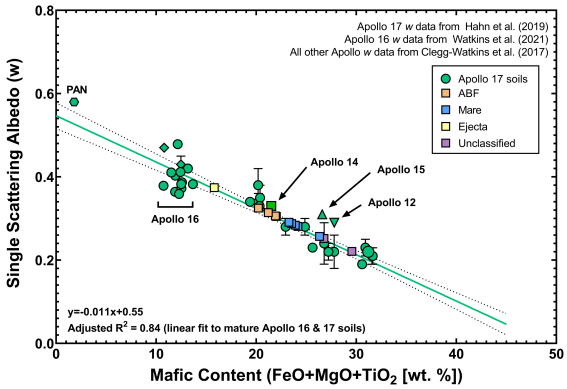

Figure 2. Single scattering albedo (*w*) and mafic mineralogy content in lunar materials as derived by [7,14,15]. Areas evaluated for this work are indicated with squares.

Photometry Results and Discussion: We extracted *w* values from 16 Regions of Interest (ROIs) across the ABF region (e.g., Fig. 1). We find that *w* ranges from 0.2 – 0.37 across the ROIs, indicating a variety of surface materials and compositions present in the region. Based on previous work by [2], we classify each surface unit as ABF material, mare, Archimedes ejecta, or "unclassified." Areas identified as ABF materials have higher *w* values than areas identified as mare, but lower *w* values than the region identified as Archimedes ejecta.

Using the relationship between *w* and mafic composition (defined here as [FeO+TiO_2+MgO] wt.%) as derived from [7,14-15] using Apollo sample data, we estimate the mafic content for each ROI in the ABF region (Fig. 2). The estimated total mafic content for the mare regions falls where expected based on the relationship between *w* and (FeO+TiO_2+MgO) determined remotely for landing site soils [14,15]. The Archimedes ejecta has the lowest mafic content of the ROIs we evaluated, consistent with lower FeO content as determined from the Clementine UV-VIS data [2].

The ABF materials are inferred to be intermediate in mafic content and *w* compared to the ejecta and mare ROIs. Thus, ABF ROIs have a lower total mafic content than the surrounding mare regions and higher total mafic content compared to crater ejecta in the region – consistent with analyses of Clementine derived FeO [2]. Thus, photometry can be used to aid in distinguishing ABF materials from nearby units at the NAC-scale, which has significantly better spatial resolution than predecessor missions.

Photometric analysis of the ABF indicates that the mafic content ranges from ~20.5-22.5 wt.% (Fig. 2). These total mafic content values are remarkably similar to what is seen in returned Apollo 15 samples. For example, sample 15205 is a fragmental or immature regolith breccia collected from a ~1 m boulder during EVA-1 that is interpreted to be local to the Apollo 15 site [5,16]. Sample 15205 is composed predominantly of KREEP basalt fragments (73% minimum [5,17]) with a total bulk rock (FeO+TiO_2+MgO) content of 21.5-24.5 wt% [5, 17-19]. Taking into account the mare basalt fragments that occur in 15205, it is likely that the total mafic content of the KREEP basalt fragments alone would prove to be an even better match to our photometry results.

Mineralogy Results and Discussion: In order to further understand the mafic mineralogy of the ABF we use the EBC and EBD of the 1 μm and 2 μm absorption features. The ABF has shallower EBDs (Fig. 3) than the surrounding mare (0.028 1μm; 0.017 2μm ABF average EBD vs. 0.059 1μm; 0.035 2μm mare average EBD), indicative of a lower mafic mineral (i.e., pyroxene, olivine) proportion, which is consistent with results from both photometry and Clementine-derived FeO, which also indicate lower mafic elements for the ABF (i.e., FeO, MgO, and TiO_2). Additionally the average EBC of the ABF is shorter than the mare (938 nm; 2044 nm ABF average EBC vs. 977 nm; 2116 nm mare average EBC). The positions of the 1 μm and 2 μm band centers indicate that the mafic mineralogy of the ABF and mare are predominantly low-Ca pyroxene, with the ABF being more Mg-rich, Ca-poor than the nearby mare. This analysis is consistent with the petrography of the Apollo 15 KREEP basalts, in which pigeonite is the most common pyroxene.

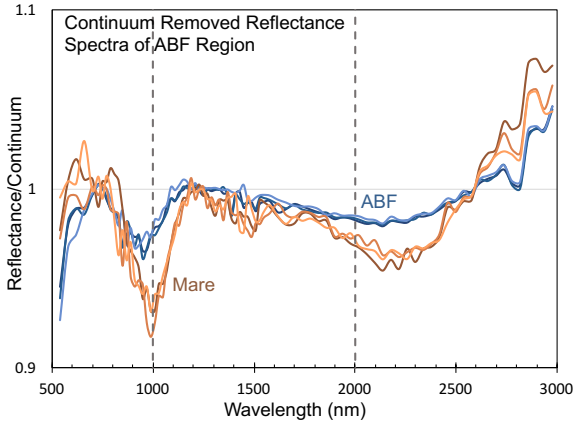

Figure 3. Representative continuum removed spectra (3×3 pixel average) of Apennine Bench Formation (blue) and nearby mare (orange).

Conclusions and Future Work: The Apennine Bench Formation likely represents the only *large* province of exposed KREEP basalts on the lunar surface. Remote sensing data from LRO and M^3 reflect the composition and mineralogy that occurs in Apollo 15 KREEP basalts, further validating that the ABF is likely volcanic and occurs at or near the Apollo 15 site. Future work includes refining our photometric and spectral analyses by including more regions of ejecta, mare, and the Apollo 15 landing site, as well as defining the "unclassified" units in consort with other remote sensing datasets (e.g., Clementine-derived FeO).

References: [1] Hackmann R. J. (1966) *Geo. Atlas of the Moon*. [2] Valencia S. N., and Jolliff B. L. (2017) *48th LPSC* abs. no. 2826. [3] Spudis P. D. (1978) *Proc. Lunar Planet. Sci. Conf. 9th*, 3379-3394 [4] Blewett D. T. and Hawke B. R. (2001) *Meteor. & Planet. Sci.,* 36, 701-730; [5] Taylor G. J., et al. (2012) *Meteor. & Planet. Sci., 47*, 861-879. [6] Hapke B. et al. (2012), *JGR-P,* 117. [7] Hahn T. M. Jr. et al. (2019) *LPSC 50* abs. no. 2132. [8] Besse S. et al. (2013) *Icarus 222*, 229-242. [9] Issacson P. J. et al. (2013) *JGRP 118*, 369-381. [10] Moriarty D. P. III and Pieters C. M. (2016)) *Meteor. & Planet. Sci*, 207-234. [11] Burns R. G. (1993) *Mineralogical Applications of Crystal Field Theory.* [12] Klima R. L. et al. (2007) *MAPS 42*, 235-253. [13] Klima R. L. et al. (2011) *Meteor. & Planet. Sci., 46*, 379-395. [14] Clegg-Watkins R. N. et al. (2017) *Icarus 285,* 169-184. [15] Watkins R. N. et al., LPSC 52.[16] Swann et al. (1972) *NASA SP-289*. [17] Simon S. B. (1986) *Geochim et Cosmochim. 50*, 2675-2691. [18] Willis J. P. et al. (1972) *The Apollo 15 lunar samples*. [19] McKay D. S. (1989) *Proc. 19th Lunar Planet. Sci. Conf.*